■ THE KNEE SOCIETY

A novel approach to 3D bone creation in minutes

3D ULTRASOUND

M. R. Mahfouz,
E. E. Abdel Fatah,
J. M. Johnson,
R. D. Komistek

From University of Tennessee, Knoxville, Tennessee, USA

Aims

The objective of this study is to assess the use of ultrasound (US) as a radiation-free imaging modality to reconstruct 3D anatomy of the knee for use in preoperative templating in knee arthroplasty.

Methods

Using an US system, which is fitted with an electromagnetic (EM) tracker that is integrated into the US probe, allows 3D tracking of the probe, femur, and tibia. The raw US radiofrequency (RF) signals are acquired and, using real-time signal processing, bone boundaries are extracted. Bone boundaries and the tracking information are fused in a 3D point cloud for the femur and tibia. Using a statistical shaping model, the patient-specific surface is reconstructed by optimizing bone geometry to match the point clouds. An accuracy analysis was conducted for 17 cadavers by comparing the 3D US models with those created using CT. US scans from 15 users were compared in order to examine the effect of operator variability on the output.

Results

The results revealed that the US bone models were accurate compared with the CT models (root mean squared error (RM)S: femur, 1.07 mm (SD 0.15); tibia, 1.02 mm (SD 0.13). Additionally, femoral landmarking proved to be accurate (transepicondylar axis: 1.07° (SD 0.65°); posterior condylar axis: 0.73° (SD 0.41°); distal condylar axis: 0.96° (SD 0.89°); medial anteroposterior (AP): 1.22 mm (SD 0.69); lateral AP: 1.21 mm (SD 1.02)). Tibial landmarking errors were slightly higher (posterior slope axis: 1.92° (SD 1.31°); and tubercle axis: 1.91° (SD 1.24°)). For implant sizing, 90% of the femora and 60% of the tibiae were sized correctly, while the remainder were only one size different from the required implant size. No difference was observed between moderate and skilled users.

Conclusion

The 3D US bone models were proven to be closely matched compared with CT and suitable for preoperative planning. The 3D US is radiation-free and offers numerous clinical opportunities for bone visualization rapidly during clinic visits, to enable pre-operative planning with implant sizing. There is potential to extend its application to 3D dynamic ligament balancing, and intraoperative registration for use with robots and navigation systems.

Cite this article: *Bone Joint J* 2021;103-B(6 Supple A):81–86.

Introduction

Osteoarthritis (OA) is a degenerative, progressive condition that affects the joints of approximately 50 million adults and 300,000 children in the USA.[1] It most commonly occurs in the knees, hips, spine, and small joints of the hands and feet. Nearly half of all Americans will develop symptoms of knee OA during their lifetime.[1] Joint pain, in general, is a major public health problem, responsible for significant costs and disability in the USA. Due at least in part to underlying OA, the direct and indirect (lost work) cost was $322 billion between 2012 and 2014.[2]

Imaging of the knee is important to help manage OA. Radiographs are important for diagnosis and surgical planning and postoperative evaluation of patients with knee OA. However,

Correspondence should be sent to M. R. Mahfouz; email: mmahfouz@utk.edu

doi:10.1302/0301-620X.103B6.BJJ-2020-2455.R1 $2.00

Bone Joint J 2021;103-B(6 Supple A):81–86.

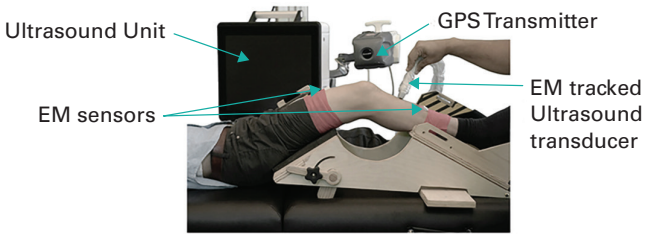

Fig. 1

System components: Ultrasound unit, Electromagnetic (EM) transmitter (GPS), EM patient tracking sensors and EM tracked ultrasound transducer.

radiographs are used while acknowledging the inherent risk of radiation exposure to the patient and clinical staff. MRI can also be used to image the knee, however its role is more limited due to longer scan time, increased cost, and incompatibility with some implants.

A major challenge for conservative management of joint pain is the lack of low-cost, accurate, radiation-free imaging. A low cost in office imaging modality to visualize joints accurately would represent a significant musculoskeletal innovation. Radiographs acquired during clinical visits are deemed the standard method for assessing joint health and are considered inexpensive, but show only joint space and osseous anatomy in a single plane. Multiple radiographs are required to view bone in different planes, but all visual assessment is conducted in 2D. Radiographs are unable to visualize directly articular cartilage, synovial bursae, menisci, ligaments, and other soft tissues involved in the development of OA. In addition, radiograph-based imaging systems (CT, radiograph, and fluoroscopy) expose patients to radiation.[3-6]

Ultrasound (US) is radiation-free and is widely accepted as a means of imaging soft tissues and joints, but not without limitations. Common US imaging techniques do not image the joint space adequately due to difficult-to-interpret 2D planar images with a limited field of view and penetration, which limits their use in orthopaedics.

As medicine moves towards patient-centred and value-based practice, preoperative planning provides valuable information to surgeons, especially when combined with 3D imaging. Potential advantages of 3D pre-surgical planning include higher accuracy compared with 2D templating,[7] and greater cost-effectiveness by reducing requested instruments and intraoperative time.[7] 3D imaging such as CT has been shown to improve surgical outcomes in different joints by enabling a more accurate diagnosis and surgical planning compared to 2D radiographs.[8]

CT and MRI are currently used in orthopaedics for reconstruction of patient-specific 3D bone models. However, little research has been conducted on the use of US in the 3D patient-specific modelling of bones and is limited to the use of brightness (B-)mode US images rather than the radiofrequency (RF) data which carry more accurate information. Barratt et al[9] and Chan et al[10] have researched the instantiation of femoral and pelvic 3D models using B-mode US. They manually extracted the bone contours from B-mode US images. Principal component analysis (PCA)-based statistical deformable models

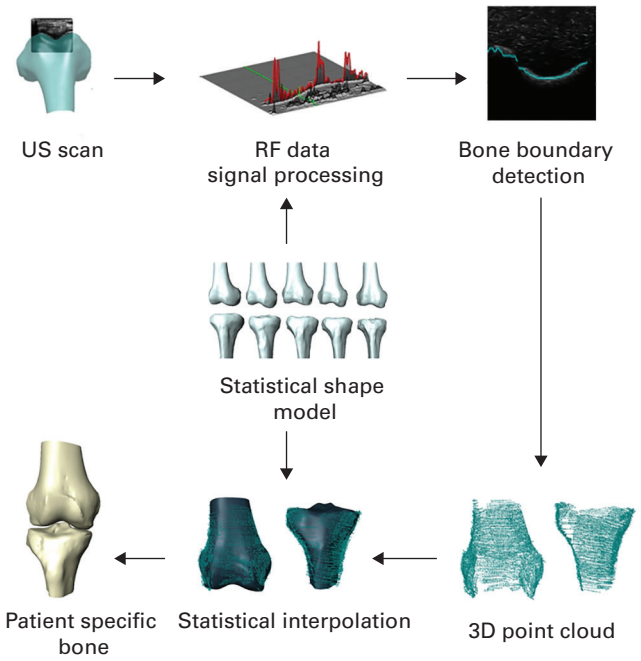

Fig. 2

An overview of the bone reconstruction algorithm. RF, radiofrequency; US, ultrasound.

(SDMs) were then used to reconstruct patient-specific bone models. Performing the experiments on three cadavers, a mean reconstruction root mean squared error (RMS) of 3.5 mm was achieved. The limitations of this work are the manual segmentation of the US images, the use of a bone-implanted reference probe, and the high reconstruction error.

Kilian et al[11] investigated the reconstruction of the distal femoral bone model using tracked B-mode US. One cadaveric distal femur was used to test the developed system and an optical motion tracking system was used for the US probe's motion tracking. The reconstruction error was specified to be less than 1 mm with local error values exceeding 2 mm at the trochlear groove and femoral condyles.

The objective of this study was to use an office-based, fully automated, real-time, noninvasive imaging system to reconstruct 3D knee models using RF US without the requirement to use a bone-implanted reference probe. In addition, we examine the accuracy of the system compared with CT and assess the feasibility of its use for preoperative planning. It is hypothesized that 3D US can be an effective alternative to radiographs for preoperative imaging during the initial preoperative appointment, making it more convenient for the surgeon and the patient.

Methods

Overview. In this study, we used a diagnostic US system directly accessing the US raw RF signals and integrated with an electromagnetic (EM) tracking system. Figure 1 outlines the system components which consist of an US unit, EM GPS transmitter, two EM sensors which are skin-mounted to the femur and

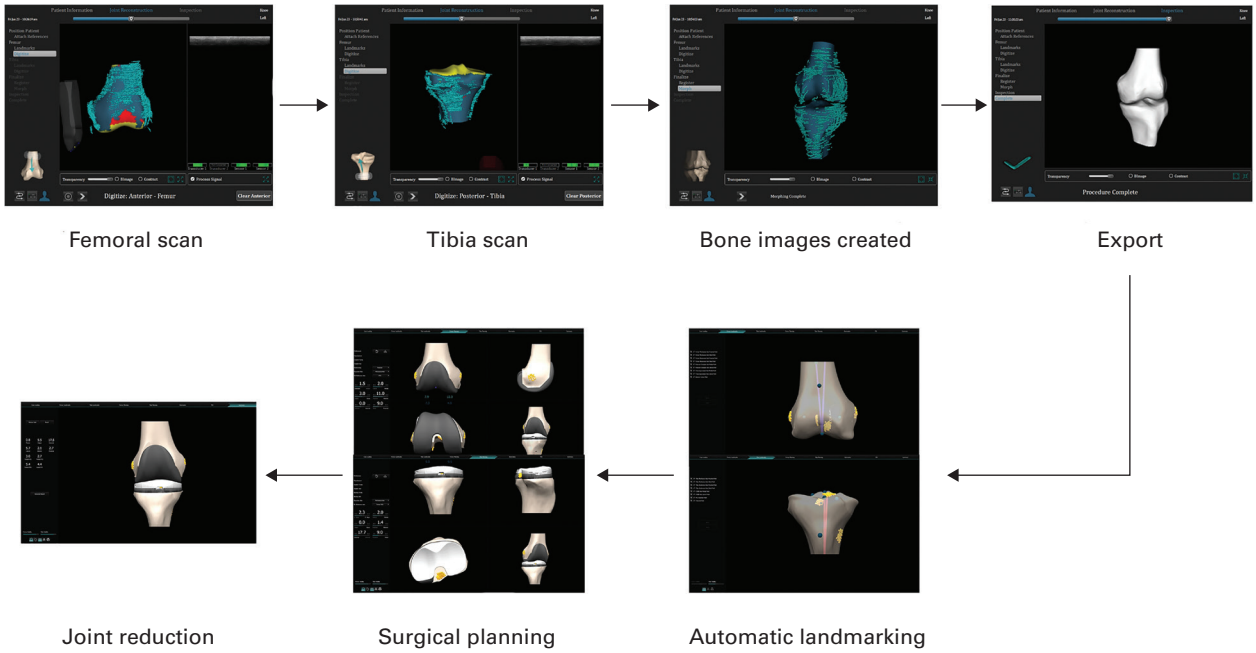

Fig. 3

Clinical workflow of model's creation using ultrasound and surgical planning.

tibia, and a linear US probe operating at 5 MHz to 14 MHz with integrated EM sensor. The EM transmitter provides a reference coordinate system where the US probe can be tracked in real time. This allows collection of spatially registered US scans. In addition, the two skin-mounted EM sensors provide the real-time location of both the femur and tibia relative to the US probe, thus allowing the system to accommodate leg motion during scanning.

We developed custom-built software that was deployed on the US unit. The software interfaces with the US unit to capture raw US RF data for processing in real time to extract bone contours. The US RF signal consists of several isolated and/or overlapping echoes. These echoes originate from the reflection of different portions of the US pulse energy at the different tissue interfaces along the US beam's path. Of these echoes, the one of interest is that generated by the bone, which arises from the reflection of the US energy at the bone surface.

The process of bone contour extraction from the US RF data frame is performed by automatically extracting the individual bone echoes from each US RF signal and then combining these individual echoes to create an image of the bone's contour. This contour is then filtered to reject outlier bone echoes and contour segments. Figure 2 outlines the 3D bone reconstruction algorithm. As the user scans the knee anatomy, the raw RF data are captured in real time, and multistage 2D and 3D signal processing algorithms are applied which filter and condition the data to compensate for loss in signal amplitude due to depth. Bone boundaries are detected from the processed data.

As the user continues scanning, contours are combined from different scan areas into 3D point clouds. Point clouds are then filtered to remove outliers. The resulting point clouds will contain gaps due to occlusion of parts of the bone by other bone.

Table I. Femoral and tibial landmarks used in comparison.

Femoral landmarks
Transepicondylar axis (TEA)
Posterior condylar axis (PCA)
Distal condylar axis (DCA)
Anterior cortex point
Anterior medial point
Anterior lateral point
Anatomical axis (FAA)
Tibial landmarks
Posterior slope axis (PSA)
Third tubercle axis (TTA)
Anatomical axis (TAA)

For example, parts of the tibial plateau are concealed by the femoral condyle and part of the trochlear groove is occluded by the patella. To fill those gaps, a statistical interpolation step is performed using statistical shape modelling (SSM).[12-14] During this iterative process, the surface of the bone is constructed from the point clouds guided by the deformable SSM acting as a 3D signal filter until the surface matches the 3D US point clouds.[15] The final relaxation step is applied to ensure the output models match the exact geometry of the 3D US point clouds. This step ensures abnormal anatomy and osteophytes are also captured in the final model. The output of the reconstruction algorithm is 3D patient-specific femoral and tibial bone models that match exactly the 3D US point clouds in areas where the data are available and approximate the anatomy in areas where the bones were occluded.

Experiments. A total of 17 cadavers were used to assess the accuracy of reconstruction compared with CT. Cadaveric specimens were thawed to room temperature and were scanned in a

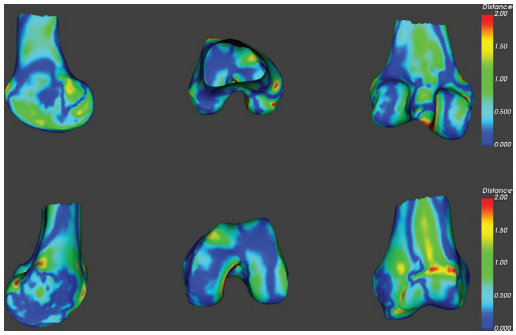

Fig. 4

Femoral surface distance map between 3D reconstruction and the CT model.

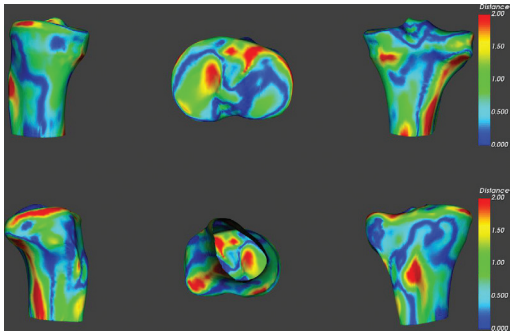

Fig. 5

Tibial surface distance map between 3D reconstruction and the CT model.

manner to replicate the clinical use of the system. 3D US was used to scan each cadaveric knee, flexed at 60°. The EM trackers were attached to the femur and tibia. The scan and clinical workflow of the system are outlined in Figure 3. The user began by scanning the femur, followed by the tibia. The 3D images created of the bones for each cadaver were then exported to the surgical planner where femoral and tibial landmarks were automatically calculated.[16-18] A list of landmarks used in the analysis can be found in Table I. Next, an analysis was performed to assess the differences between the 3D bone models generated from CT (using the process of segmentation) and those created using US. A statistical evaluation was conducted on various parameters to assess the error.

Error analysis. Comparison between the US- and the CT-generated 3D bone models was performed as follows: register CT to US model using iterative closet point (ICP);[12] compute the landmarks outlined in Table I for the CT models, in addition to the mechanical axis which was calculated as the line joining the femoral head and joint centre;[16-18] compute surface-to-surface statistics between each pair of CT and US models by finding the distance between each point on the US model and the closest point on the CT surface (use the statistics to compute the RMS error); for each set of models, an anatomical coordinate system was established. The mechanical axis of the CT data was used to define the proximal/distal direction.

The following differences in landmarks and orientation of relevant clinical axes were calculated: for femoral transepicondylar axis (TEA) and posterior condylar axis (PCA) (difference in internal/external rotation); for distal condylar axis (difference in varus/valgus); medial anteroposterior (AP) distance (MAP); lateral AP distance (LAP); difference in tibia posterior slope axis (PSA); difference in internal/external rotation of the medial one-third of the tibial tubercle to posterior cruciate ligament (PCL) attachment point (third tubercle axis (TTA)); calculate the difference in implant size between the US and CT models for both femur and tibia.

Interobserver study. Usability of the system and the effect of user experience level on the accuracy of the system was evaluated using 15 users with varying US experience (unskilled (no previous US experience and introductory anatomy knowledge) to expert (previous US experience and in depth knowledge of anatomy)). Each user completed at least one complete scan of a knee phantom. Surgical landmarks were then calculated on the output femoral and tibial models for each user and the ground truth phantom CT models. The angular differences between femur (TEA, PCA, and FAA) and tibia (TTA and TAA) were then calculated.

Statistical analysis. Given the nature of our analysis, we choose to use the one-sample *t*-test for equivalence to examine the equivalency between the 3D models created from the US system and those created from CT. An equivalency interval of 1.5 mm was adopted which is an acceptable margin of error for preoperative planning application and intraoperative guidance. PASS 2020 software (NCSS, USA) was used to perform power analysis using the independent-samples *t*-test equivalence procedure using an α of 0.05 on both femoral and tibia RMS error.

For the accuracy, analysis descriptive statistics were calculated including mean and standard deviation (SD) for each measurement.

To examine the output of the interobserver study, NCSS 2020 was used to perform one-way analysis of variance (ANOVA) using Kruskal-Wallis ANOVA on ranks and the Kruskal-Wallis multiple-comparison z-value test. The level of statistical significance was set at a p-value < 0.05.

Results

The accuracy comparison performed on 17 cadaveric specimens revealed that US bone models were comparable with CT models with a power value of 99% and 100% for femur and tibia, respectively. The mean for femur RMS error was found to be 1.07 mm (SD 0.15), and 1.02 mm (SD 0.13) for the tibia. Figure 4 and Figure 5 show examples of a surface-to-surface error map for the femur and tibia, respectively, for a cadaveric specimen. Differences in the orientation of surgical axes in the femur and tibia for the 17 cadavers (Table II) were found to be TEA axis: 1.07° (SD 0.65°); PCA: 0.73° (SD 0.41°); and DCA: 0.96° (SD 0.89°). In addition, examining the difference, MAP was 1.22 mm (SD 0.69), whereas LAP was 1.21 mm (SD 1.02). Tibial landmarking errors were slightly higher than those noted for the femur with mean difference in posterior slope axis of 1.92° (SD 1.31°) and 1.91° (SD 1.24°) for the one-third tubercle axis. Figure 6 shows the comparison of landmarks for one of the cadaveric specimens between CT and US. In all, 90% of the femora and 60% of the tibiae were

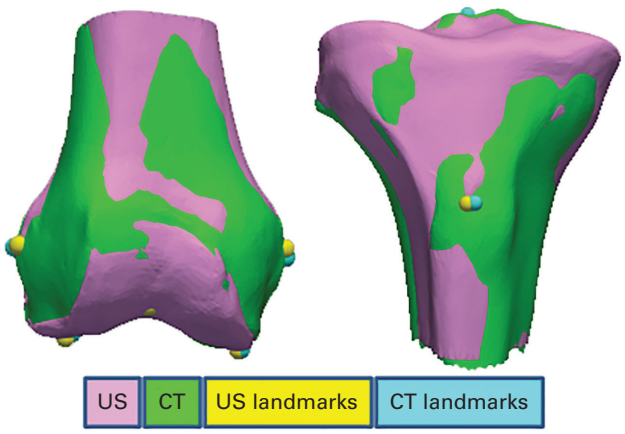

Fig. 6

Comparison of CT (green) and ultrasound (magenta) femoral and tibial landmarks. US, ultrasound.

found to have the same size in both CT and US, while 10% of the femora and 40% of the tibiae were found to have one size difference between CT and US.

For the interobserver study, 15 users were classified into three categories: unskilled; moderate; and expert, based on their familiarity with US. Figure 7 shows the mean error in surgical axes alignment between different user groups. The Kruskal-Wallis on ranks and the Kruskal-Wallis multiple-comparison z-value test showed no statistical difference between the outputs of each of the user groups ($p = 0.050$).

Discussion

In this work we presented a real-time knee imaging system for automatic reconstruction of patient-specific 3D bone models using US, and explored the potential clinical impact of the system by evaluating surface and landmark discrepancies with those found on CT scanning. With surface discrepancies near 1 mm and clinical landmarks well localized, the models from the system performed well, with all components from the surgical planning exercise correct to within one size, when using the CT scans as the reference standard. Additionally, the effect of user experience on the outcome of the system was evaluated and showed no statistical difference in the output models between users with different levels of experience. It has been demonstrated that even segmentation from CT is prone to variability,[19] which is why it is important to achieve consistency in results across users.

The accuracy of this system is in line with clinical need, specifically to support surgical planning, as demonstrated by the accuracy of the experiment results. In addition, surface error accuracy has demonstrated the potential to use the system to guide placement of injections. Another benefit of this system is that the entire workflow of imaging, bone reconstruction, and planning could be performed in one visit and improve efficiency. One of the criticisms for 2D US pertains to the fact that well trained, experienced sonographers must be used because the transducer is held by hand during most US procedures. The details of acquisition, including the view angle, significantly

Table II. The mean difference in landmarks for femur and tibia (n = 17 cadavers) between the CT and ultrasound-generated models.

Measurement	Mean difference (SD)
Femur	
TEA, °	1.07 (0.65)
PCA, °	0.73 (0.41)
DCA, °	0.96 (0.89)
MAP, mm	1.22 (0.69)
LAP, mm	1.21 (1.02)
Tibia	
PSA, °	1.92 (1.31)
TTA, °	1.91 (1.24)

DCA, distal condylar axis; LAP, lateral anteroposterior length; MAP, medial anteroposterior length; PCA, posterior condylar axis; PSA, posterior slope axis; SD, standard deviation; TEA, transepicondylar axis; TTA, third tubercle axis.

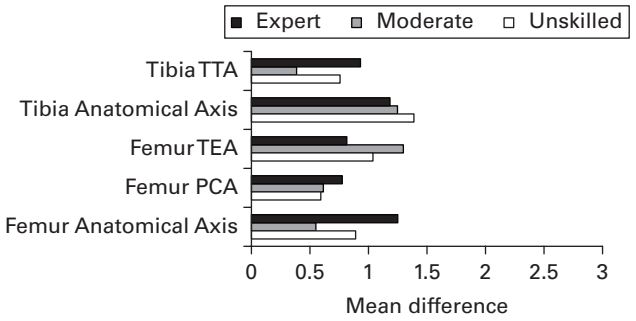

Fig. 7

Mean difference in landmarks between ultrasound and CT categorized by user skillset. PCA, posteriorcondylar axis; TEA, transepicondylaraxis; TTA, third tubercle axis.

influence both the field of view and the image quality, which makes operator experience the main factor in imaging modality effectiveness.[20] With an automated guided reconstruction, the system eliminated the need for operator interpretation of the B-mode images, which is a major step in simplifying the procedure. The encouraging results of the interobserver study suggest the potential to expand the use of the system to a wider group of clinicians with variable expertise.

Limitations of this work include use of cadaveric specimens only, which are different in temperature to a patient population. This discrepancy must be accounted for and may affect US accuracy. Some previous studies have even attempted to calibrate for speed of sound when in an unknown medium.[21] Additionally, cadavers may vary greatly in terms of tissue quality and are likely not representative of an osteoarthritic patient population in obesity or level of bone pathology.

Another limitation was the use of a single linear US transducer. Switching to a lower-frequency curvilinear transducer may yield better results as it would provide a signal capable of penetrating deeper into the tissue. This is important for evaluating the posterior aspects of the femur. The intraobserver study sample size was limited to five individuals per group; an increase in the number of participants in each group in future studies would provide greater statistical power.

While our study does not specifically address the dynamic imaging element of the system, we have shown promising results for establishing a radiation-free, on-site imaging system for building 3D models of the knee and have shown that those models are sufficient for pre-surgical planning. It is unlikely that radiographs, CT, and MRI will be entirely replaced by the US system, but we believe we have demonstrated that there is an opportunity to reduce the use of ionizing radiation. Additionally, further development may enable a preoperative appreciation of the periarticular soft-tissues. Future work seeks to improve the system by increasing accuracy through various methods, including upgrading the imaging and tracking systems, and using US harmonics to enhance the bone contour detection. Various software improvements have been undertaken to increase the reproducibility, such as automatically detecting when a scan has been completed sufficiently to yield acceptable results.

Use of US has thus far been limited in the field of joint replacement. The system outlined may offer a clinically applicable, non-ionizing radiation method for imaging bone.

Take home message

- 3D ultrasound (US) offers numerous clinical opportunities for bone creation in minutes during their office visit, surgeon-patient preoperative planning, 3D dynamic ligament balancing and intraoperative registration for use with robots and navigation systems.
- Bone models created from 3D US are accurate when compared to CT.

References

1. **No authors listed**. What is arthritis? Arthritis Foundation. 2020. https://www.arthritis.org/health-wellness/about-arthritis/understanding-arthritis/what-is-arthritis (date last accessed 30 November 2020).
2. **Weistein SI**, **Yelin EH**, **Watkins-Castillo SI**. The burden of musculoskeletal diseases in the United States. United States bone and joint initiative. 2020. https://www.boneandjointburden.org/fourth-edition/ij0/summary-and-conclusions (date last accessed 18 March 2021).
3. **Brenner DJ**, **Hall EJ**. Computed tomography--an increasing source of radiation exposure. *N Engl J Med*. 2007;357(22):2277–2284.
4. **Goldman LW**. Principles of CT: radiation dose and image quality. *J Nucl Med Technol*. 2007;35(4):213–225.
5. **Berrington de González A**, **Darby S**. Risk of cancer from diagnostic X-rays: estimates for the UK and 14 other countries. *Lancet*. 2004;363(9406):345–351.
6. **Ron E**. Ionizing radiation and cancer risk: evidence from epidemiology. *Pediatr Radiol*. 2002;32(4):232–237.
7. **Ettinger M**, **Claassen L**, **Paes P**, **Calliess T**. 2D versus 3D templating in total knee arthroplasty. *Knee*. 2016;23(1):149–151.
8. **Leung KH**, **Fang CX**, **Lau TW**, **Leung FK**. Preoperative radiography versus computed tomography for surgical planning for ankle fractures. *J Orthop Surg*. 2016;24(2):158–162.
9. **Barratt DC**, **Chan CSK**, **Edwards PJ**, **et al**. Instantiation and registration of statistical shape models of the femur and pelvis using 3D ultrasound imaging. *Med Image Anal*. 2008;12(3):358–374.
10. **Chan CSK**, **Barratt DC**, **Edwards PJ**, **Penney GP**. 2004. Cadaver validation of the use of ultrasound for 3D model Instantiation of bony anatomy in image guided orthopaedic surgery. *Medical Image Computing and Computer-Assisted Intervention -- MICCAI 2004, 7th International Conference Saint-Malo, France, September 26-29, 2004, Proceedings, Part II* 397–404.
11. **Kilian P**, **Plaskos C**, **Parratte S**, **et al**. New visualization tools: computer vision and ultrasound for MIS navigation. *Int J Med Robot*. 2008;4(1):23–31.
12. **Mahfouz MR**, **Merkl BC**, **Fatah EEA**, **Booth R**, **Argenson JN**. Automatic methods for characterization of sexual dimorphism of adult femora: distal femur. *Comput Methods Biomech Biomed Engin*. 2007;10(6):447–456.
13. **Mahfouz MR**, **Badawi A**, **Merkl B**, **et al**. Patella sex determination by 3D statistical shape models and nonlinear classifiers. *Forensic Sci Int*. 2007;173(2-3):161–170.
14. **Mahfouz MR**, **Mustafa A**, **Abdel Fatah EE**, **Herrmann NP**, **Langley NR**. Computerized reconstruction of fragmentary skeletal remains. *Forensic Sci Int*. 2017;275:212–223.
15. **Mahfouz MR**. Method and apparatus for three-dimensional reconstruction of a joint using ultrasound, patent No. US20130144135A1. https://patents.google.com/patent/EP2600766A1/en (date last accessed 20 April 2021).
16. **Mahfouz MR**, **Abdel Fatah EE**, **Merkl BC**, **Mitchell JW**. Automatic and manual methodology for three-dimensional measurements of distal femoral gender differences and femoral component placement. *J Knee Surg*. 2009;22(4):294–304.
17. **Mahfouz M**, **Abdel Fatah EE**, **Bowers LS**, **Scuderi G**. Three-dimensional morphology of the knee reveals ethnic differences. *Clin Orthop Relat Res*. 2012;470(1):172–185.
18. **Mahfouz MR**, **ElHak Abdel Fatah E**, **Bowers L**, **Scuderi G**. A new method for calculating femoral anterior cortex point location and its effect on component sizing and placement. *Clin Orthop Relat Res*. 2015;473(1):126–132.
19. **Van den Broeck J**, **Vereecke E**, **Wirix-Speetjens R**, **Vander Sloten J**. Segmentation accuracy of long bones. *Med Eng Phys*. 2014;36(7):949–953.
20. **Delzell PB**, **Boyle A**, **Schneider E**. Dedicated training program for shoulder sonography: the results of a quality program reverberate with everyone. *J Ultrasound Med*. 2015;34(6):1037–1042.
21. **Mehrdad S**, **Prevost R**, **Moctezuma J-L**, **Navab N**, **Wein W**. 2017. Precise ultrasound bone registration with learning-based segmentation and speed of sound calibration. *International Conference on Medical Image Computing and Computer-Assisted Intervention. Springer. MICCAI*. 682–690.

Author information:
M. R. Mahfouz, PhD, Professor of Biomedical Engineering
E. E. Abdel Fatah, PhD, Research Assistant Professor
R. D. Komistek, PhD, Professor of Biomedical Engineering
Mechanical, Aerospace, and Biomedical Engineering Department, University of Tennessee, Knoxville, Tennessee, USA.

J. M. Johnson, PhD, Vice President of Operation and Development, TechMah LLC, Knoxville, Tennessee, USA.

Author contributions:
M. R. Mahfouz: Analyzed the data, Prepared the manuscript.
E. E. Abdel Fatah: Analyzed the data, Prepared the manuscript.
J. M. Johnson: Analyzed the data, Prepared the manuscript.
R. D. Komistek: Analyzed the data, Prepared the manuscript.

Funding statement:
No benefits in any form have been received or will be received from a commercial party related directly or indirectly to the subject of this article.

ICMJE COI statement:
M. R. Mahfouz reports receipt of a grant from the University of Tennessee, related to this study, and payment to his institution for Board membership of JointVue LLC, receipt of institutional grant(s) from the University of Tennessee, payment to his institution for patent(s) from JointVue LLC, and stock options received from JointVue LLC, all unrelated to this study. E. E. Abdel Fatah reports receipt of an institutional grant from UTK, related to this study. J. M. Johnson reports employment by Techmah LLC and stock options received from JointVue LLC, all unrelated to this study. R. D. Komistek reports Board membership of JointVue LLC and receipt of stock options from same, all unrelated to this study.

This article was primary edited by G. Scott.

This paper was presented at The Knee Society 2020 Members Meeting, held virtually.